AFOSR 2304

DESLIP IN ALUMINUM SINGLE CRYSTAL SPECIMENS

(Terminal Report)

by

Robert B. Pond

Eleanor Harrison

The Johns Hopkins University

January 1962

SOLID STATE SCIENCES DIVISION

AIR FORCE OFFICE OF SCIENTIFIC RESEARCH

ARDC

Washington 25, D. C.

Contract No. AF 49 (638)-509

ABSTRACT

By the technique of interferometric cinemicrography which was developed on this contract deslip in aluminum single crystals was observed as a result of reversing the stress. An explanation of the phenomenon is presented.

The technique is also used to evaluate the effects of temperature over the range -150°F to +225°F, on the velocity of slip.

Unslip of a band during continuing deformation was observed and an explanation of the phenomenon is presented.

INTRODUCTION

Investigations of the plastic deformation of metals can be divided into three general areas by considering the physical scale the investigations incorporate. These three groups are a) the submicroscopic, b) the microscopic, and c) the macroscopic. Investigations of the submicroscopic type are concerned with the basic structure, dislocations and other imperfections and their behavior under plastic deformation. Such investigations have been principally concerned with static tests although in recent years dynamic observations have been accomplished. Investigations of the macroscopic type are concerned with geometric shape of the specimen, strain rate effects, stress-strain relationships, strain wave propagation, and so forth. Such investigations comprise the bulk of the efforts so far expended in the general field and have involved both static and dynamic observations. Investigations of the microscopic type are concerned with crystal class and orientations, grain boundary effects, slip bands, deformation bands, twins and so forth. Such investigations, although numerous, have been principally carried out by static observations. Dynamic observations of the microscopic behavior of a metal being plastically deformed have been reported by Chen and Pond (1), Becker and Haasen (2), Haasen and Siems (3) and Pond and Harrison (4). Because of the scarcity of such dynamic observations an array of data in excess of the amount necessary to present this report is included so the

scientific community can have access to it.

The technique of interferometric cinemicrography (5) which was developed under this contract was used in the documentation hereafter presented.

SPECIMEN PREPARATION

All specimens used in these investigations were cast aluminum single crystals 1/8 inch x 1/8 inch square in cross section by 1-3/8 inches long in gauge length and were produced from research purity (99.99% pure) aluminum by a modified Bridgman process. This process which was described by Chen and Pond (1) was used to produce 108 crystals simultaneously from the same melt. By gating from the foot of each crystal to a common seed large numbers of crystals having the same orientation and purity were produced.

Each crystal was ground flat, etched, thermally homogenized and, finally, electrolytically polished in methyl alcohol and nitric acid (2/1). The crystallographic orientations were determined by the Laue X-ray back-reflection method. From this data the side of the crystal was selected on which the maximum surface upheaval would result from primary slip. This side of the crystal was used for microscopic observation. The orientations relative to the specimen axis or stress axis are presented in Fig. 1-A for the specimens used in the deslip experiments and in Fig. 1-B for the temperature experiments.

METHOD OF TESTING AND DEVELOPING DATA

After each crystal was prepared and immediately before it was tested the interference mirror was attached to the selected side. The crystal was then placed in the micro tensile machine on the microscope as previously described (1) and in the case of the deslip experiments it was first compressed and then extended, the interval of time between the reversal being controlled. In all other cases the specimen was simply extended. During deformation the motion picture record was made of the changes occurring in the interference pattern. The camera speed was 12 frames per second. The minimum vertical resolution by the interference pattern was 100 Å and the minimum lateral resolution of the microscope was .0022 mm.

High temperature runs were accomplished by encapsulating the specimen on the three sides not used for observation in a small Nichrome heater. Low temperature runs were accomplished by packing crushed dry ice around the specimen and grips. The interference mirror and the objective lens were kept free by means of an aluminum foil shield which was wrapped around the objective tube and the specimen at the point of observation. In both cases the temperature was determined by means of a thermocouple situated on the specimen.

Following each successful run the film was developed and that portion of the film was printed which depicted the phenomenon from the beginning of slip on the first slip band until sufficient

slip bands had appeared so that the field became confused. These prints were analyzed by measuring the average "elevation factor" for each line at many different times (or at many different strain intervals). The "elevation factor" is defined as the ratio of the extent of displacement of an interference fringe to the distance between fringes and is that factor which, when multiplied by $1/\cos\theta$ (where θ is the angle between the normal to the observation plane and the slip direction) and multiplied by the half wave length of the radiation used, equals to the resolved shear or extent of slip in the slip direction. An illustration of a resulting plot is given in Figs. 2, 3, 4. From such a plot the velocity of slip can be determined for each slip band at any time or extent of strain desired.

PRESENTATION OF RESULTS

This investigation was conducted in two parts. The first part was concerned with endeavors to deslip aluminum. The second part was concerned with temperature effects on the velocity of slip. In order to prevent confusion the results will be presented and discussed independently.

1. Deslip

A summary tabulation of the data developed during these investigations is not revealing since it is awkward to insert in such a tabulation the juxtaposition of the slip lines. The data is therefore presented in two forms. Figs. 6, 7, 8 and 9 illustrate

a) the relative spatial positions of the array of slip bands by ordinate intercepts, b) the time during which slip occurred on each band by the abcissa interval of the cross-hatched area, c) the velocity of slip by the height of the cross-hatched area, d) the extent of slip by the area of the cross-hatched area, e) the time of compressive load cessation by noting as Reversal, f) the interval of time after compression before tensile extension.

It can be noted in Fig. 6 that after maintaining a compressive stress on the specimen 9-1-5 for 5.58 seconds the load was removed and after a wait of 38.2 seconds a tensile stress was applied which resulted in deslipping on the compressive bands C_1, C_2, C_3, and C_4.

Deslip was not observed on every slip band nor was deslip observed in every specimen. In most instances the tensile bands developed were interspersed between the compressive bands. This resulted in extrusions and metallurgical notches. So that the extent of such notches and extrusions can be appreciated the results of the reversed stress are presented in time-distance extent of gliding plots in Figs. 10, 11, 12, and 13. The profiles herein presented are the physical surfaces of the observation surface as seen in the plane containing the stress axis and the slip directions.

Although such plots delineate the juxtaposition of tensile and compressive slip bands the history of deslip is not adequately presented. Fig. 14 illustrates similar profiles taken at various time intervals for specimen 9-1-5. The extent of compressive slip,

deslip, and tensile slip on the same band is easily observed in this plot.

No correlation could be made between deslip and any other factor such as a) orientation, b) extent of slip, c) velocity of slip, rapidity of stress reversal, etc.

2. Temperature Effects

The specimens used in these tests are identified with a three part index, i.e. 39-3-16. The first number (39) identifies the heat or the gang of crystals simultaneously produced. The second number (3) identifies the orientation, and the last number (16) identifies the specific specimen. Interferometric cinemicrographic tests were performed at the three temperature levels, approximately -150°F, room temperature and approximately 225°F.

Tables 1 thru 9 present the data illustrating the chronological appearance of the slip bands, the extent of slip, and the velocity of slip. The slip line number frequently contains a subscript number which indicates whether the shear referred to is the first, second, etc., shear observed on this band. A better understanding of this multiple movement on the same band can be had by studying Fig. 2. The slopes of the lines in Fig. 2 are the velocities of slip. These same velocities are presented in bar graph form in Fig. 16.

During some of the high temperature extensions some slip bands seemed to partially disappear. This phenomenon is hereafter referred to as "Unslip" and is illustrated in Fig. 15. At the end

of these specific runs the load was maintained constant for a period of time and photographs taken before unloading. Fig. 15 shows further unslip on one band during this interval. Fig. 5 at room temperature and Fig. 2 at low temperature indicate no unslip.

All of the data from these investigations has not been presented. The reason for these omissions is one of the following: a) picture out of focus, b) insufficient fringes in the field to allow accurate measurement, or c) fringes too fuzzy to allow precise measurement.

DISCUSSION OF RESULTS

1. Deslip

The time records of slip developed have all shown the velocity of slip to be a constant with no acceleration or deceleration apparent. This fact led to the supposition that strain hardening on the slip band is cataclysmic and requires some finite period of time. It was further supposed that if the stress could be reversed within this period of time it should be possible to deslip the material.

The current investigations have not shown this time dependence to exist. Fig. 6 illustrates the fact that a slip band may cease to be active after about two seconds (line C1) and yet it can be deslipped after a wait of 41 seconds.

The evidence that an aluminum single crystal can be deslipped is not to be doubted. Yet it was not possible to deslip all of the

active slip bands in the specimens in which deslip was observed. It also proved to be impossible to detect any deslip in the records from some specimens. Efforts were made to correlate the tendency to deslip with orientation and extent of compressive strain without success. The deslip phenomenon can be explained by lattice bending as is discussed under temperature effects.

2. Temperature Effects

The slip velocities observed at the various temperatures follow the law previously presented (4)

$$V = K\dot{\epsilon}\left(\frac{\sigma^2}{2Ef}\right)$$

where K is a constant presently not understood but probably related to dislocation density

$\dot{\epsilon}$ - Strain rate

σ - Elastic Limit stress

E - Elastic modulus in direction of stress axis

f - Frequency of coactive slip bands

The elastic limit stress change over the temperature range varies from 124 gm/mm^2 at the low temperature to 92 gm/mm^2 at the high temperature as the Elastic Modulus changes from 9×10^6 gm/mm^2 at the low temperature to 6×10^6 gm/mm^2 at the high temperature. The $\frac{\sigma^2}{2E}$ factor therefore varies from 8.5×10^{-4} to 7.0×10^{-4}. The distance between coactive slip bands (1/f) on the other hand is observed to vary between 5 and 100 microns.

Since these tests were performed at approximately the same strain rate it would be expected that the velocity of slip could

change by two orders of magnitude as a function of the frequency of coactive slip bands alone. It would also be expected that the elastic resilience would not affect the velocity to any noticeable extent. In general the low temperature slip velocities are observed to have higher values than those obtained in the high temperature tests. The distance between the coactive bands can be greater in the low temperature tests than in the high temperature tests. This is necessarily a qualitative statement in view of the fact that the coactive band frequency can change by an order of magnitude in one specimen at a given temperature.

One of the most unexpected observations of this investigation is that of unslip. An explanation of this may be found by consideration of Fig. 17. If a total slip band does not become active at one time, one of two possible configurations must exist. Either the lattice between the slip planes must be bent as illustrated or one end of the crystal must twist about the specimen axis relative to the other end. In the case where the dislocation loops penetrate the surface in the center of the specimen the twisting is not possible and lattice bending must occur. If this lattice bending is of an elastic type, it is possible that a slip band becoming active in its close proximity can relieve the load and elastic restitution can occur or unslipping can occur as a result of released elastic strains.

It is also speculated that this bent lattice concept can explain the deslip when the stress is purposefully reversed. Since the elastic bending will provide an incremental and highly directed additive stress to the reversed stress, the bands which would deslip would only be those which were associated with lattice bending.

CONCLUSIONS

1. It is possible to deslip aluminum single crystals with reversed stresses.
2. The deslip phenomenon is not dependent on time, extent of strain, or orientation, but may be dependent on lattice bending.
3. The velocity of slip in the temperature range between -150°F and 225°F is relatively unaffected by the mechanical property changes.
4. The velocities of slip in the afore mentioned temperature range are primarily dependent on the frequency of co-active slip bands.
5. It is possible for a slip band to unslip or partially restore itself to its original configuration without a stress reversal or while slip is continuing on other bands.
6. Unslip can be explained by lattice bending of the elastic type.

ACKNOWLEDGMENT

The authors wish to acknowledge and express their gratitude for the efforts of Mr. Carol Mobley. His careful measurements and dedicated efforts have reduced a myriad of photomicrographs to a sensible array of data.

TABLE 1
Al 39-3-12
+77°F
12 frames/sec.

Line	Ratio	Resolved Shear(A)	Glide Time (Seconds)	Time from Beginning of Run(sec)	Time between Lines(sec)	Velocity A/sec
1_1	.130	418				
2^1_1	.160	515				
3^1_1	.057	184	Lines in at beginning of run			
4^1_1	.135	434				
5^1_1	.027	87				
4^1_2	.045	145	.25	1.00		580
6^2_1	.040	129	.42	1.08	.08	307
4^1_3	.017	55	.10	1.50	.42	550
4^3_4	.013	42	.08	2.00	.50	525
5^4_2	.020	64	.18	2.82	.82	355
4^2_5	.015	48	.09	3.08	.26	533
6^5_2	.055	177	.42	4.65	1.57	422
5^2_3	.020	64	.17	4.75	.10	376
7^3_1	.035	113	1.00	10.00	5.25	113
8^1_1	.030	97	.25	10.90	.90	388
6^1_3	.040	129	.80	15.05	4.15	161
8^3_2	.022	71	.23	16.42	1.37	309
6^2_4	.037	119	.36	16.82	.40	331
8^4_3	.078	251	.65	17.70	.88	386
6^3_5	.028	90	.15	18.42	.72	600
7^5_2	.030	97	.22	19.08	.66	441
8^2_4	.025	81	.15	19.25	.17	540
7^4_3	.030	97	.18	19.92	.67	539
2^3_2	.030	97	.15	22.50	2.58	647
5^2_4	.040	129	.65	22.52	.02	198
6^4_6	.022	71	.25	24.25	1.73	284
6^6_7	.033	106	.32	24.75	.50	331

TABLE 2
Al 39-6-1
+77°F
12 frames/sec.

Line	Ratio	Resolved Shear A	Glide Time(sec)	Time from Beginning of run(sec)	Time between Lines(sec)	Velocity A/sec
1_1	.495	2145				
2^1	.225	977				
3^1	.252	1093	Lines in at beginning of run			
4^1	.125	543				
5^1_1	.295	1281	1.15	7.0		1114
1^1_1	.070	304	0.40	7.60	0.60	760
6^2	.135	586	1.35	7.90	0.30	434
5^1_1	.105	456	0.50	9.55	1.65	912
6^2	.162	703	0.50	9.63	0.08	1406
3^2_2	.038	165	0.15	10.15	0.52	1100
3^2_3	.030	130.3	0.12	10.50	0.35	1086
6^3	.068	295	0.30	10.52	0.02	984
3^2_4	.060	260.5	0.15	11.60	1.08	1735

TABLE 3
Al 39-3-16
+235-225°F
12 frames/sec.

Line	Ratio	Resolved Shear(A)	Glide Time (Seconds)	Time from Beginning of Run(sec)	Time between Lines(sec)	Velocity A/sec
1_1	.168	541				
2_1	.040	129				
3_1	.030	97				
4_1	.075	242		Lines in at beginning of run		
5_1	.108	348				
6_1	.025	81				
7_1	.045	145				
6_2	.040	129	.25	7.17		516
2_2	.160	515	.50	8.17	1.00	1030
2_3	.058	187	.25	9.07	.90	748
6_3	.040	129	.30	9.50	.43	430
2_4	.042	135	.28	10.35	.85	482
7_2	.090	290	.23	10.85	.50	1260
3_2	.202	651	.42	13.43	2.58	1550
7_3	.105	338	.70	13.80	.37	483

TABLE 4
Al 39-6-7
230-225°F
12 frames/sec

Line	Ratio	Resolved Shear(Å)	Glide Time (Seconds)	Time from Beginning of Run(sec)	Time between Lines(sec)	Velocity Å/sec
1_1	.517	2245	Lines in at beginning of run			
2_1	.385	1670				
3_1	.200	867	0.33	1.67		2625
4_1	.300	1302	1.04	3.78	2.11	1252
5_1	.095	412	0.50	4.15	0.37	824
2_1	-.107	-464	0.45	4.30	0.15	1032
3_1	-.040	-174	0.15	5.45	1.15	1160
3_2	-.035	-152	0.15	5.92	0.47	1013
2_2	.040	174	0.25	6.00	0.08	696
3_3	-.020	-87	0.13	6.35	0.35	669
2_3	.036	156	0.15	6.52	0.17	1040
3_4	-.030	-130	0.17	6.93	0.41	765
5_1	-.028	-122	0.15	7.50	0.57	814
3_5	-.025	-108	0.17	7.83	0.33	635
6_1	.062	269	0.15	8.10	0.27	1793
5_2	-.022	-95	0.20	8.68	0.58	475
3_6	-.020	-87	0.08	9.00	0.32	1088
6_2	.038	165	0.28	9.22	0.22	589
2_4	.052	226	0.20	9.30	0.08	1130
2_5	.068	295	0.27	10.15	0.85	1093
5_3	-.025	-108	0.17	11.25	1.10	635
5_4	-.020	- 87	0.25	12.18	0.93	348
2_6	.054	234	0.30	13.05	0.87	780
7_1	.143	621	0.68	15.07	2.02	914
2_7	.074	321	0.27	16.00	0.93	1188
7_2	.102	442	0.50	17.38	1.38	884
6_3	.120	521	0.38	17.42	0.04	1371
2_8	.093	403	0.35	19.40	1.98	1152
7_3	.047	204	0.15	20.65	1.25	1360
4_2	.055	239	0.32	20.95	0.30	747
6_4	.085	369	0.33	22.10	1.15	1119
8_1	.050	217	0.35	26.40	4.30	620

TABLE 5
Al 39-6-5
230°F-225°F
12 frames/sec.

Line	Ratio	Shear °A Resolved	Glide Time(sec)	Time from beginning of run(sec)	Time between lines(sec)	Velocity A/sec
1_1	.212	919				
2_1	.280	1214				
3_1	.072	312	Lines in at beginning of run			
4_1	.048	208				
5_1	.045	195				
2_2	.035	152	0.30	0.17		507
6_1	.050	217	0.20	0.72	.55	1084
4_2	.057	247	0.17	0.75	.03	1452
3_2	.173	750	0.23	0.77	.02	3260
7_1	.040	173	0.28	0.82	.05	618
6_2	.105	456	0.35	1.92	1.10	1301
1_2	.085	369	0.31	1.97	.05	1190
4_3	.115	498	0.25	2.00	.03	1992
8_1	.075	325	0.65	2.10	.10	500
5_2	.155	672	0.50	2.25	.15	1344
3_3	.085	369	0.25	2.43	.18	1476
4_4	.135	586	0.30	2.52	.09	1951
7_2	.028	121	0.15	2.62	.10	807
5_3	.033	143	0.15	3.67	1.05	954
6_3	.065	282	0.25	3.75	.08	1128
1_3	.058	252	0.13	3.87	.12	1939
3_4	.065	282	0.30	3.95	.08	940
6_4	.030	130	0.10	5.45	1.50	1300
9_1	.042	182	0.30	5.55	.10	607
1_4	.120	521	0.23	5.80	.25	2262
3_5	.030	130	0.15	5.92	.12	867
6_5	.050	217	0.17	6.00	.08	1276
5_4	.092	399	0.47	6.10	.10	849
10_1	.190	824	0.38	8.52	2.42	2165
5_5	.128	555	0.28	8.52	0.00	1982
11_1	.093	403	0.27	8.55	.03	1493
12_1	.045	195	0.15	8.85	.30	1300
6_6	.060	260	0.25	9.10	.25	1040
11_2	.152	659	0.30	10.00	.90	2195
13_1	.045	195	0.15	10.03	.03	1300
12_2	.048	208	0.13	10.12	.09	1600
10_2	.055	239	0.20	10.50	.38	1195
12_3	.067	291	0.30	10.52	.02	970
11_3	.040	173	0.19	10.73	.21	911
6_7	.108	468	0.25	10.75	.02	1872
11_4	.107	464	0.48	11.20	.45	968
13_2	.080	347	0.40	11.35	.15	868

TABLE 5 (Continued)

Line	Ratio	Shear • A Resolved	Glide Time(sec)	Time from beginning of run(sec)	Time between lines(sec)	Velocity A/sec
14_1	.160	694	0.55	11.68	.33	1261
6^1	.097	421	0.34	11.93	.25	1238
10^8_3	.187	811	0.33	12.05	.12	2455
15^3_1	.155	672	0.20	12.15	.10	3360
16^1_1	.048	208	0.15	12.92	.77	1387
10^1_4	.088	382	0.45	13.00	.08	848
15_2	.033	143	0.30	13.20	.20	477
17^2_1	.080	347	0.28	13.22	.02	1239
18^1_1	.045	195	0.23	13.32	.10	848
19^1_1	.036	156	0.15	13.43	.11	1040
19_2	.086	373	0.37	13.93	.50	1008
16^2_2	.104	451	0.31	14.52	.59	1453
17^2_2	.165	716	0.22	14.60	.08	3250
9^2_2	.053	230	0.25	14.75	.15	920

TABLE 6
Al 39-3-13
-120°F
12 frames/sec

Line	Ratio	Resolved Shear A	Glide Time(sec)	Time from Beginning of run(sec)	Time between Lines(sec)	Velocity A/sec
1_1	.150	483				
2_1	.070	226		Lines in at beginning of run		
3_1	.040	129				
4_1	.260	837	.75	1.25		1116
5_1	.020	64.4	.18	1.50	.25	358
6_1	.043	138	.15	1.75	.25	920
7_1	.110	354	.55	2.05	.30	644
8_1	.100	322	.50	2.75	.70	644
6_2	.017	55	.08	3.92	1.17	688
7_2	.060	193	.12	4.13	.21	1610
8_2	.053	171	.25	4.75	.62	684
6_3	.035	113	.20	5.17	.42	565
9_1	.027	87	.18	6.57	1.40	483
8_3	.082	264	.25	6.75	.18	1056
8_4	.045	145	.20	7.55	.80	725
9_2	.070	226	.35	8.60	1.05	646
10_1	.170	547	.78	9.72	1.12	702
5_2	.070	226	.45	9.80	.08	502
11_1	.220	709	.75	9.85	.05	945
12_1	.025	80.5	.05	9.87	.02	1610
13_1	.165	532	.80	9.95	.08	665
12_2	.155	499	.35	10.15	.20	1427
14_1	.100	322	.58	10.17	.02	555
15_1	.047	151	.20	10.32	.15	755
10_2	.105	338	.30	10.70	.38	1127
11_2	.050	161	.18	10.82	.12	895
13_2	.055	177	.25	12.00	1.18	708
5_3	.022	71	.13	12.07	.07	546
15_2	.028	90.3	.23	12.07	.00	393
14_2	.058	187	.40	12.10	.03	467
14_3	.030	97	.18	12.82	.72	539
14_4	.030	97	.17	13.25	.43	570

TABLE 7
Al 60-39-9-1
-158°F
32 frames/sec.

Line	Ratio	Resolved Shear Å	Glide Time(sec)	Time from Beginning of run(sec)	Time between Lines(sec)	Velocity Å/sec
1_1	.03	130				
2_1	.185	803	Lines in at beginning of run			
1_2	.245	1063	.09	0.88	0.88	11815
3_1	.055	238	.125	0.94	0.06	1903
4_1	.285	1237	.08	4.56	3.62	15470
2_2	.030	130	.13	4.57	0.01	1000
5_1	.035	152	.045	4.585	0.015	3375
3_2	.150	651	.045	4.59	0.005	14450
6_1	.030	130	.06	4.615	0.025	2165
7_1	.512	2220	.075	6.06	1.445	29600
8_1	.030	130	.04	6.075	0.015	3250
9_1	.165	716	.075	6.12	0.045	9545
1_3	.060	260	.075	6.32	0.20	3465
9_2	.140	607	.10	6.75	0.43	6070

TABLE 8
Al 39-9-3
-190°F
32 frames/sec

Line	Ratio	Resolved Shear(Å)	Glide Time (Seconds)	Time from Beginning of Run(sec)	Time between Lines(sec)	Velocity Å/sec
1_1	.242	1050	.105	.21		10000
2_1	.190	824	.045	.28	.07	18310
3_1	.107	464	.025	.315	.035	18580
3_2	.173	751	.13	.78	.465	5775
2_2	.077	334	.05	.80	.02	6685
4_1	.378	1640	.05	.85	.05	32800
$5\text{-}6_1$	.360	1562	.16	1.50	.65	9760
$5\text{-}6_2$	.141	612	.12	2.12	.62	5100
3_3	.042	182	.035	2.65	.53	5200
$5\text{-}6_3$	.125	542	.075	2.775	.125	7235
2_3	.043	187	.045	2.825	.050	4160
7_1	.200	868	.11	2.85	.025	7890
2_4	.030	130	.035	3.34	.49	3715
7_2	.073	317	.04	3.35	.01	7925
8_1	.232	1007	.08	3.40	.05	12590
3_4	.058	252	.02	3.41	.01	12600
8_2	.100	434	.065	4.065	.655	6685
8_3	.268	1162	.10	4.80	.735	11620
3_5	.060	261	.035	4.95	.15	7460
9_1	.177	768	.14	5.39	.44	5485
8_4	.110	477	.03	5.45	.06	15910
3_6	.047	204	.065	5.50	.05	3140
10_1	.055	239	.06	5.50	.00	3980
10_2	.055	239	.065	7.025	1.525	3680

TABLE 9
Al 39-2-3
-155°F
32 frames/sec

Line	Ratio	Resolved Shear A	Glide Time (sec)	Time from Beginning of Run(sec)	Time between Lines(sec)	Velocity A/Sec
1_1	.126	1328				
2^1	.080	843	Lines in at beginning of run			
3^1	.040	421				
4^1	.357	3760				
3^1	.160	1687	.07	.23		24100
5^2	.215	2265	.09	.31	0.08	25200
5^1	.077	812	.07	.44	0.13	11600
2^2	.020	211	.04	.50	0.06	5275
5^2	.041	432	.025	.80	0.30	17290
5^3	.034	358	.035	1.98	1.18	10220
6^4	.205	2160	.09	2.11	0.13	24000
6^1	.045	474	.14	2.84	0.73	3385
6^2_3	.057	601	.10	7.09	4.25	6010

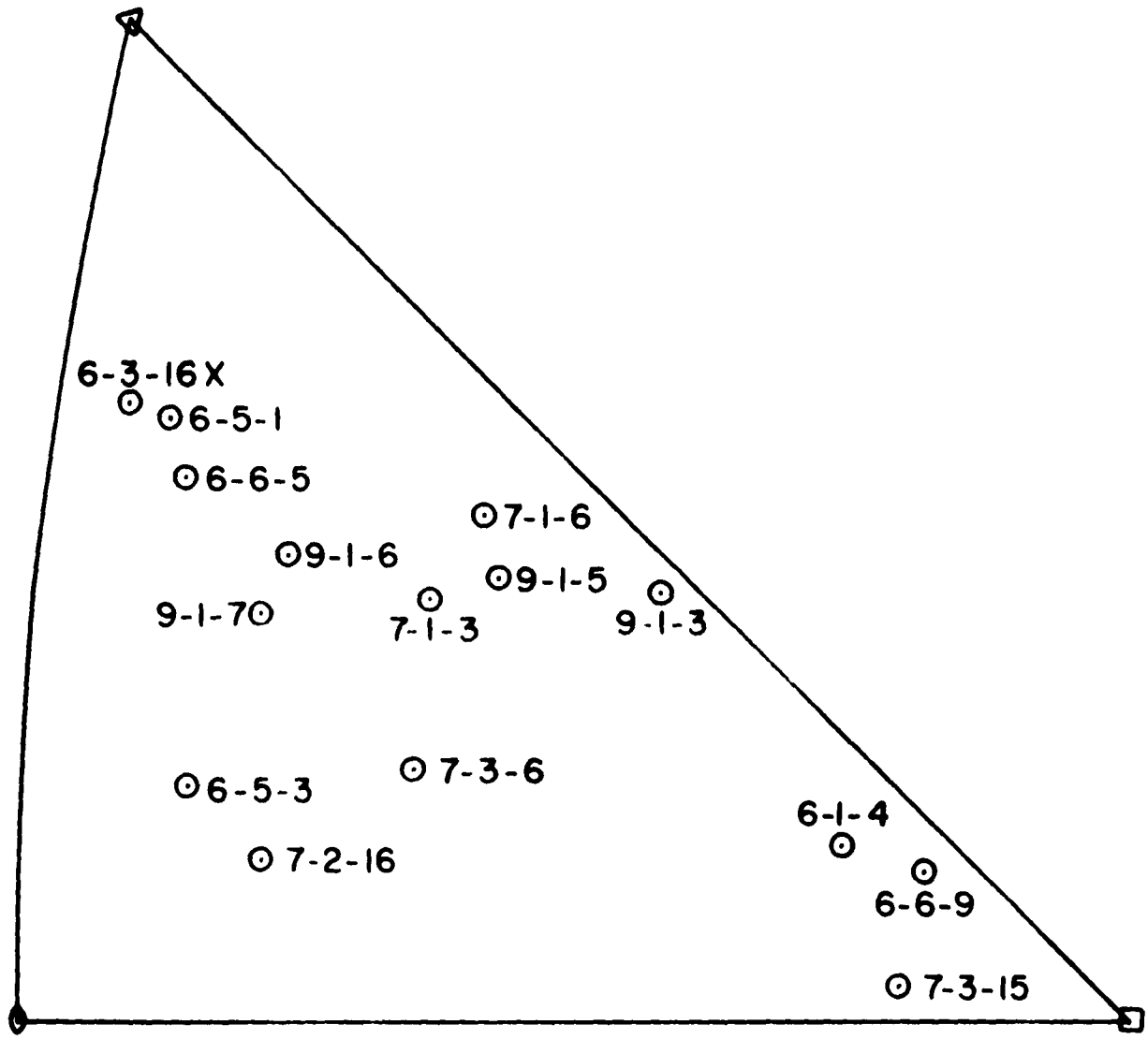

Figure 1a

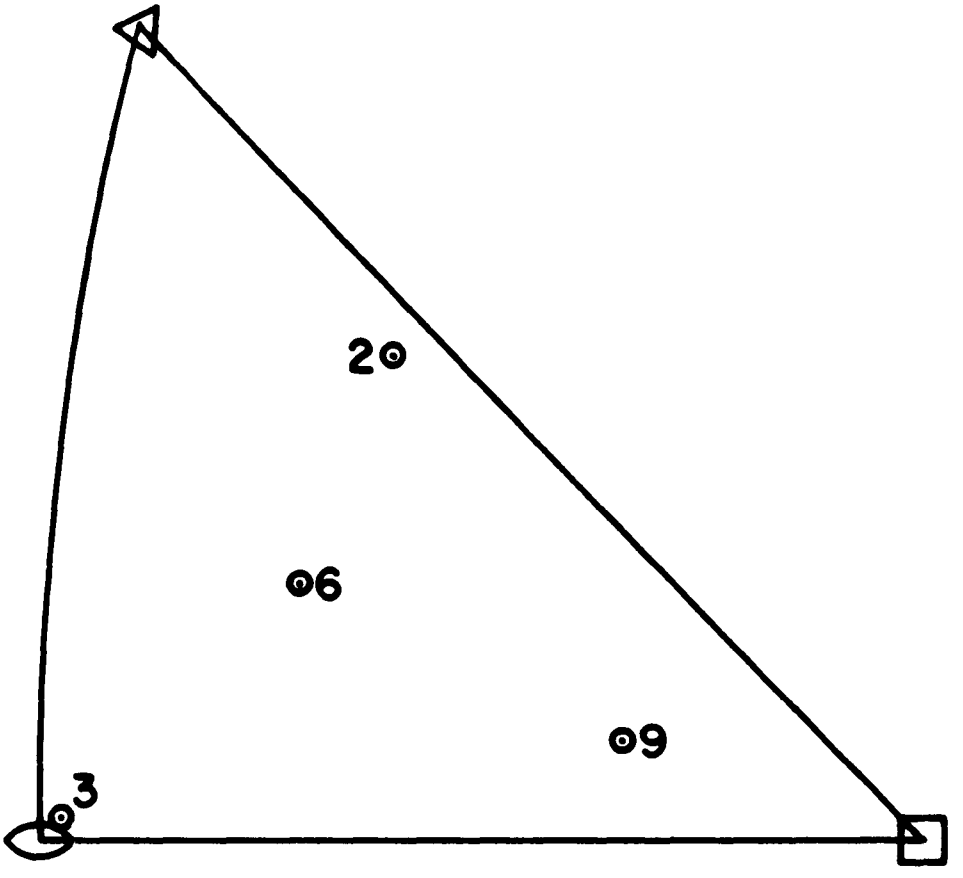

FIG. 1b

RESOLVED SHEAR, ANGSTROMS
2500
2000
1500
1000
500
0
AL 39-6-5
TIME, SECONDS
0
1
2
3
4
5
6
7
8
9
10
11
12
13
14
15
58
59
BREAK IN RUN FROM 18.33 SEC. TO 57.33 SEC.
RUN ENDS AT 58.91 SEC.

FIG. 2

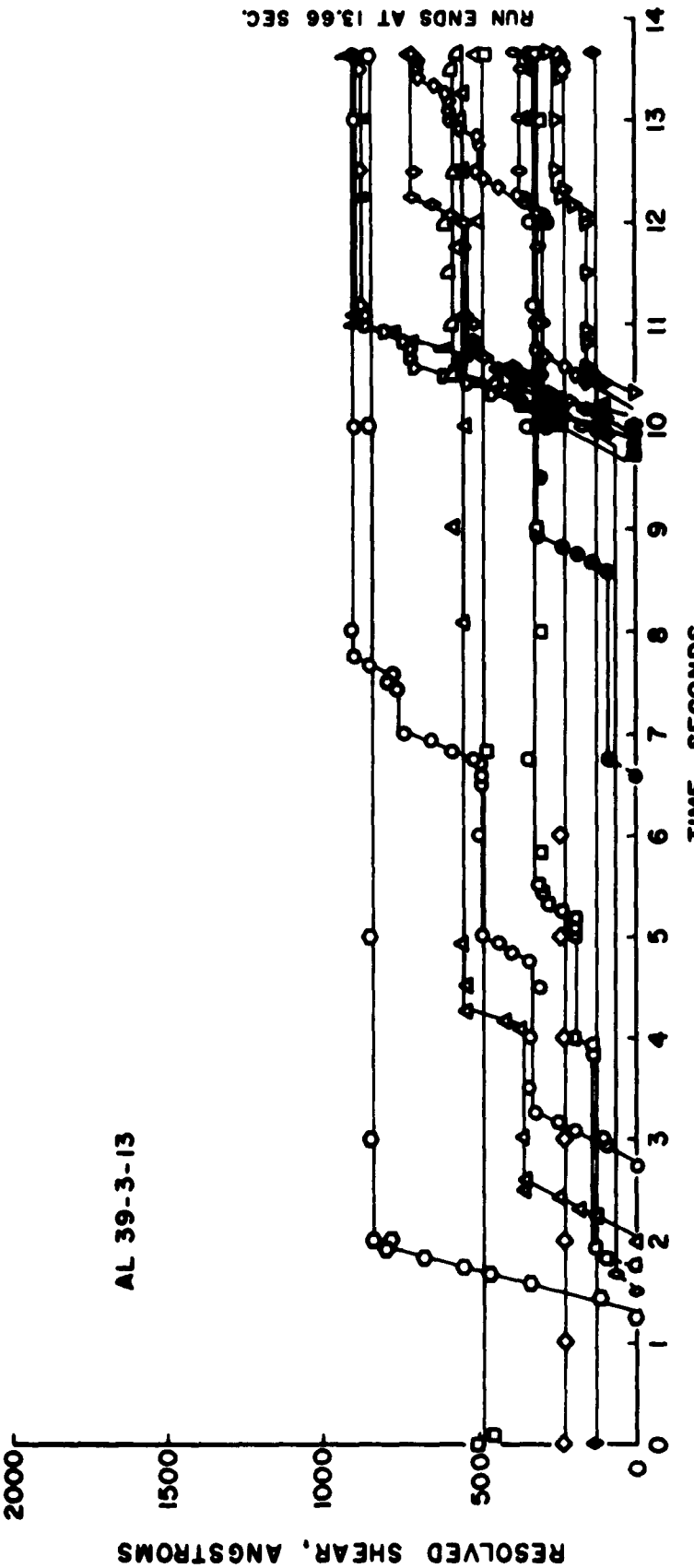
RUN ENDS AT 13.66 SEC.
AL 39-3-13
RESOLVED SHEAR, ANGSTROMS
2000
1500
1000
500
0
0
1
2
3
4
5
6
7
8
9
10
11
12
13
14
TIME, SECONDS

FIG. 3

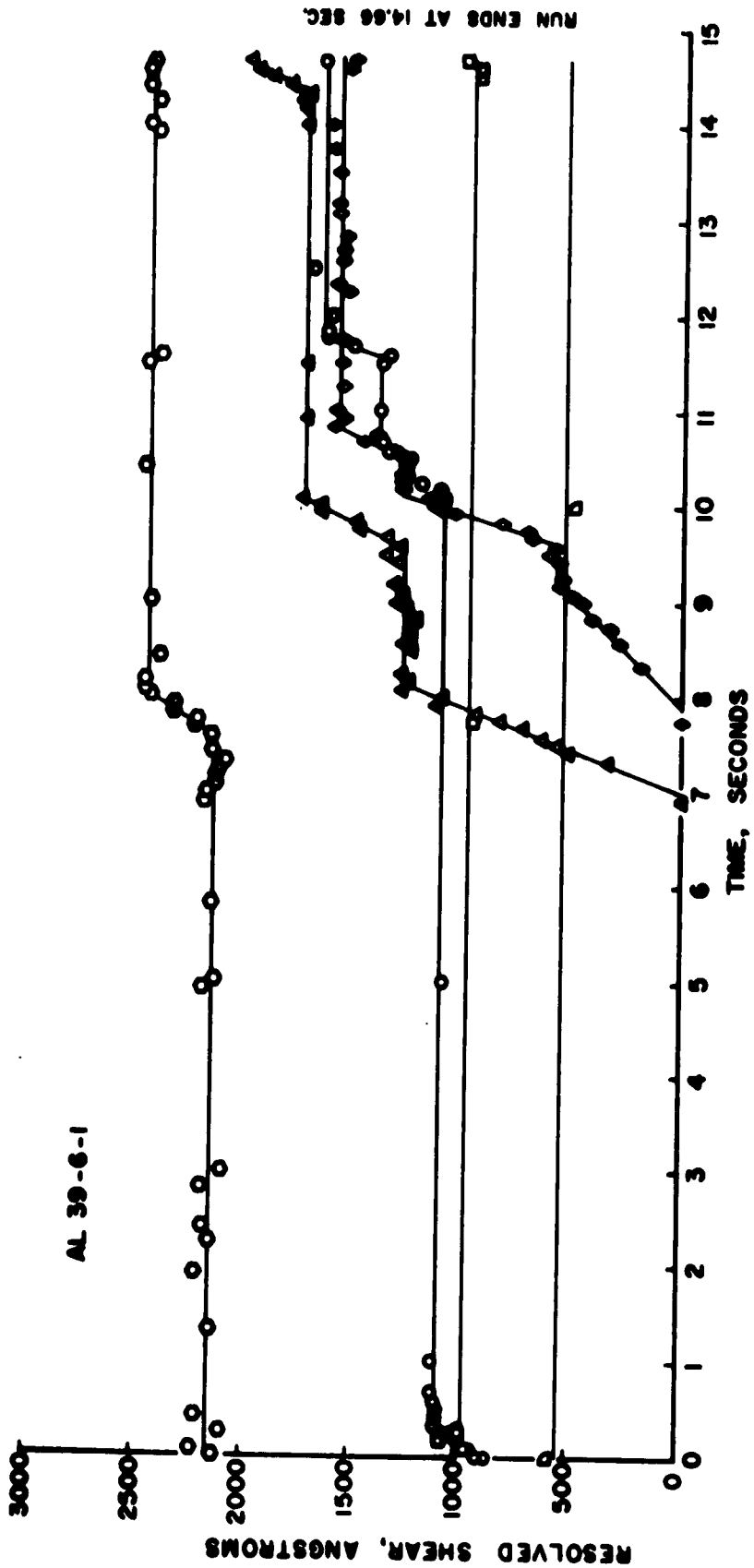
RUN ENDS AT 14.66 SEC.
AL 39-6-1
RESOLVED SHEAR, ANGSTROMS
3000
2500
2000
1500
1000
500
0
0
1
2
3
4
5
6
7
8
9
10
11
12
13
14
15
TIME, SECONDS

FIG. 4

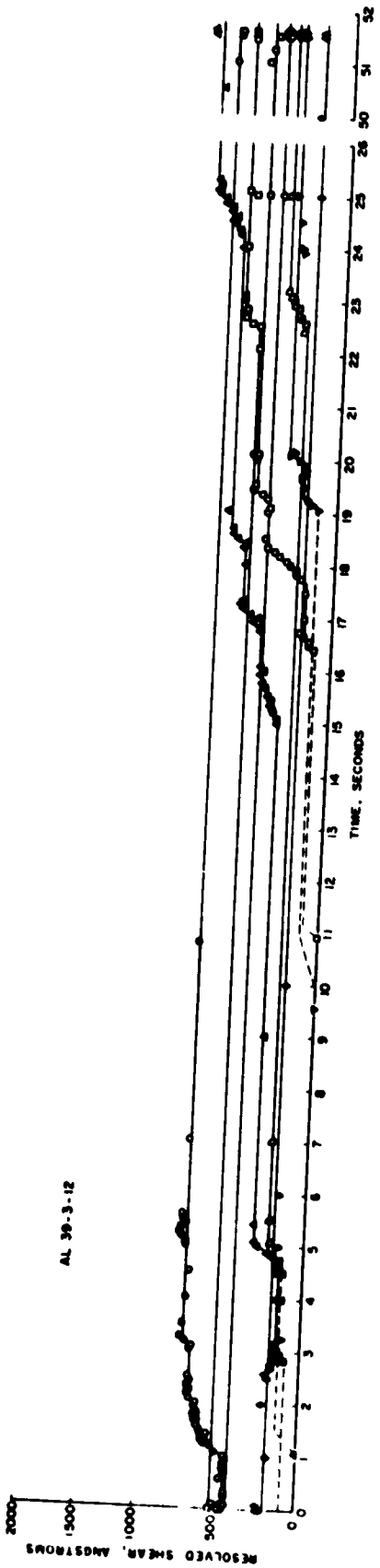
AL 39-3-12
RESOLVED SHEAR, ANGSTROMS
2000
1500
1000
500
0
TIME, SECONDS
0
1
2
3
4
5
6
7
8
9
10
11
12
13
14
15
16
17
18
19
20
21
22
23
24
25
26
50
51
52

FIG. 5

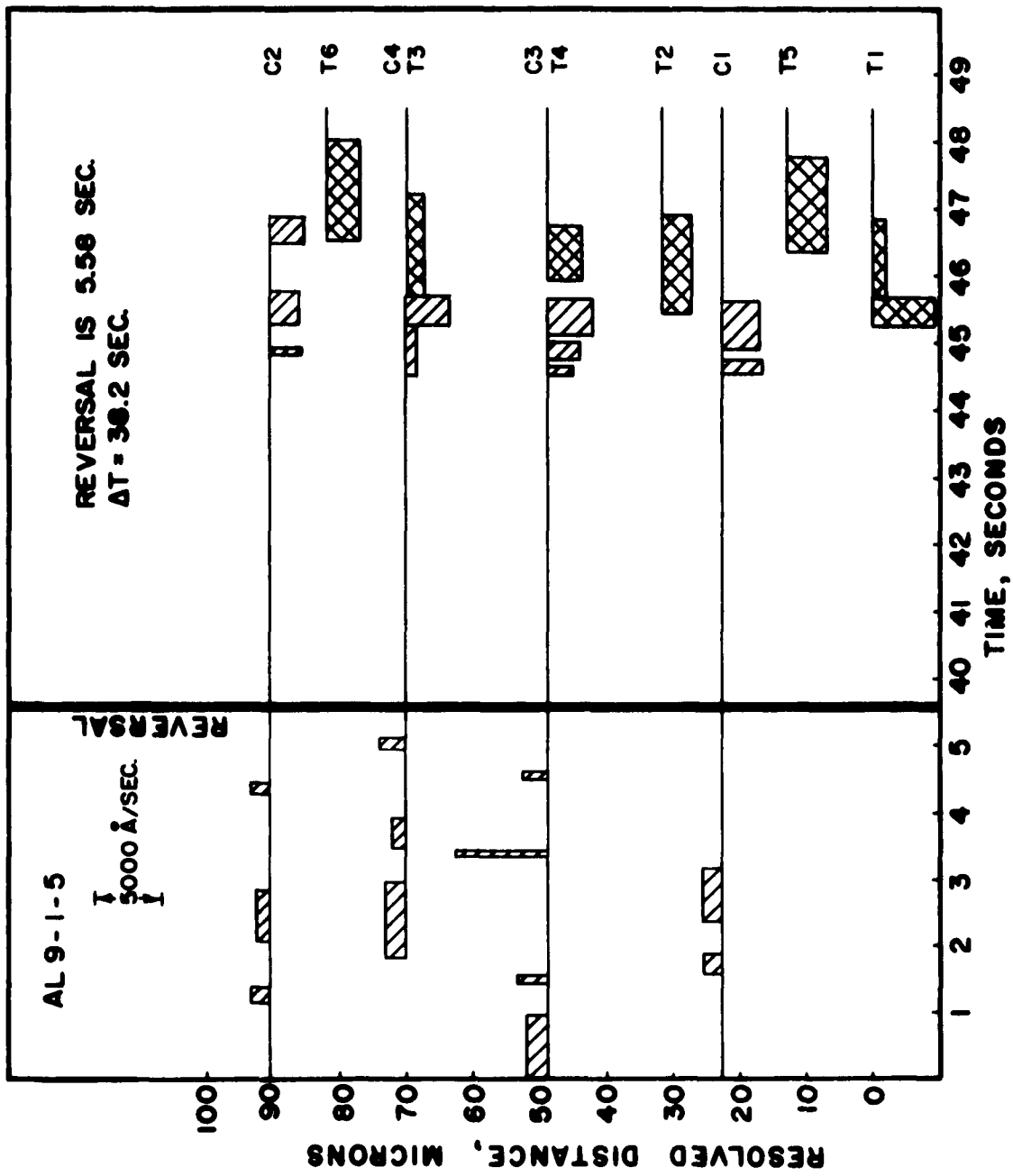
AL 9-1-5
5000 Å/SEC.
REVERSAL
REVERSAL IS 5.58 SEC.
ΔT = 38.2 SEC.
C2
T6
C4
T3
C3
T4
T2
C1
T5
T1
RESOLVED DISTANCE, MICRONS
TIME, SECONDS

FIG. 6

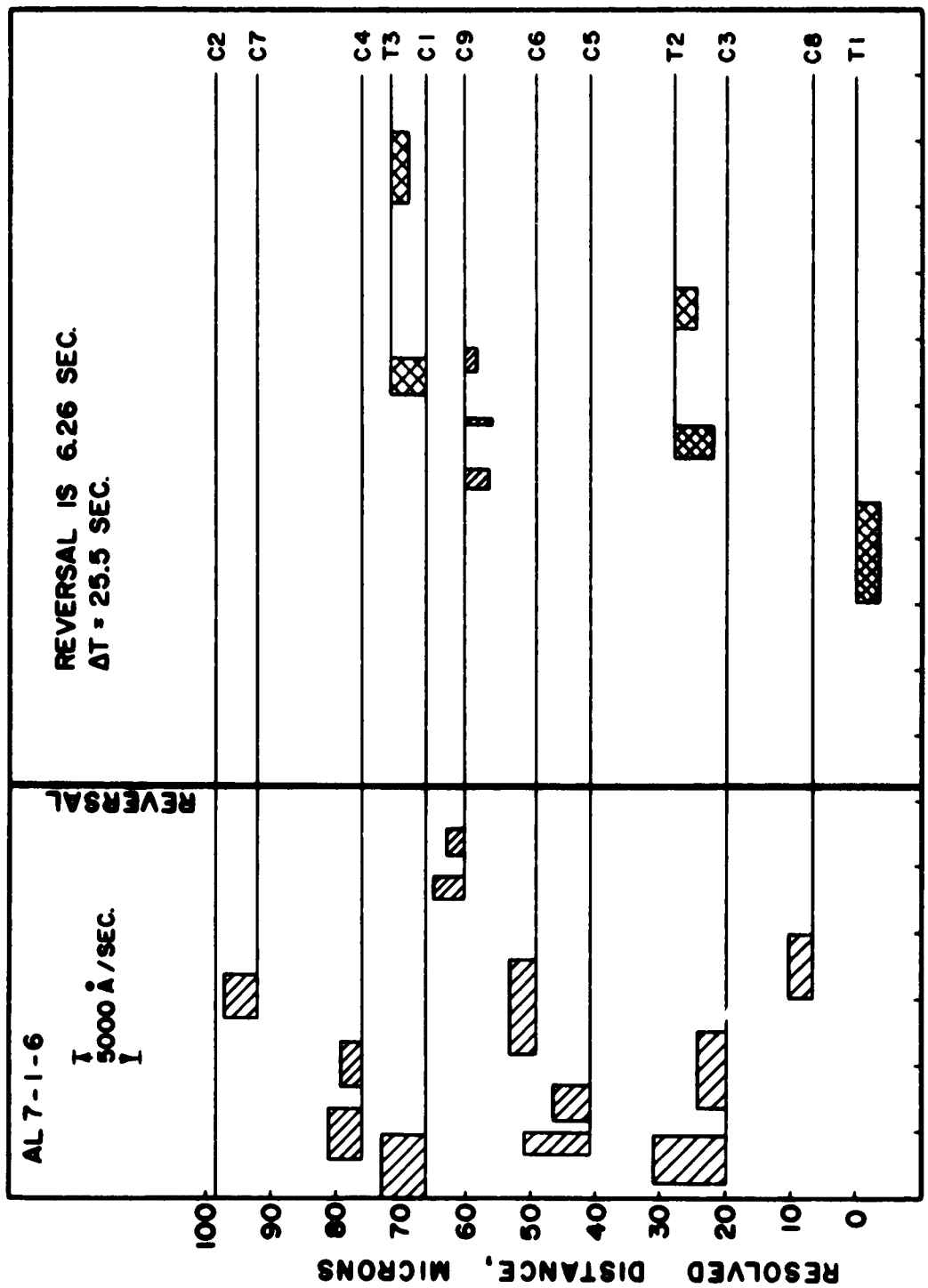
AL 7-1-6
5000 Å/SEC.
REVERSAL
REVERSAL IS 6.26 SEC.
ΔT = 25.5 SEC.
C2
C7
C4
T3
C1
C9
C6
C5
T2
C3
C8
T1
100
90
80
70
60
50
40
30
20
10
0
RESOLVED DISTANCE, MICRONS
1
2
3
4
5
6
30
31
32
33
34
35
36
37
38
39
40
TIME, SECONDS

FIG. 7

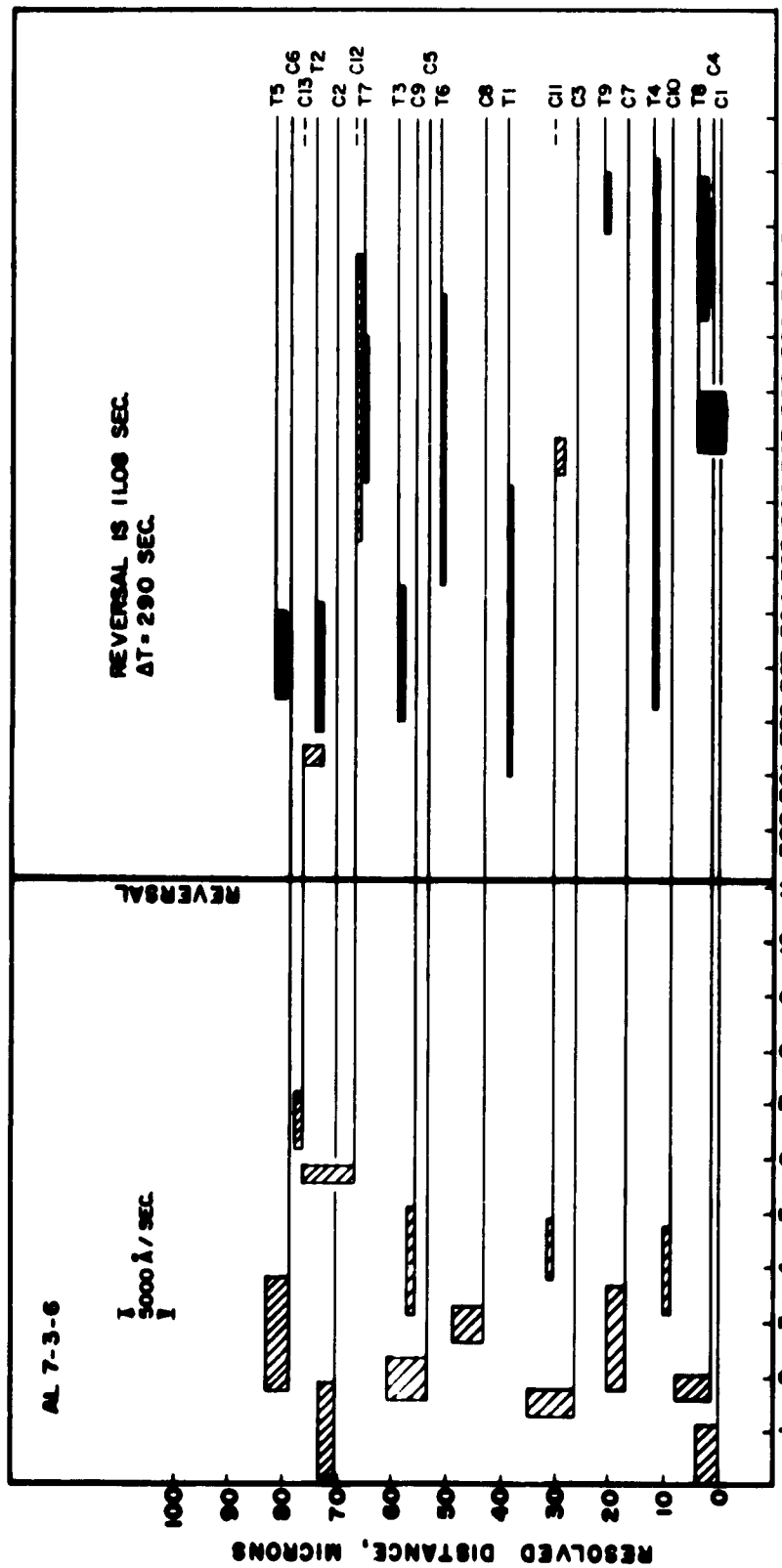
AL 7-3-6
5000 Å / SEC
REVERSAL
REVERSAL IS 1108 SEC.
ΔT = 290 SEC.
T5 C6
C13 T2
C2 C12
T7
T3
C9 C5
T6
C8
T1
C11
C3
T9
C7
T4
C10
T8 C4
C1
RESOLVED DISTANCE, MICRONS
TIME, SECONDS

FIG. 8

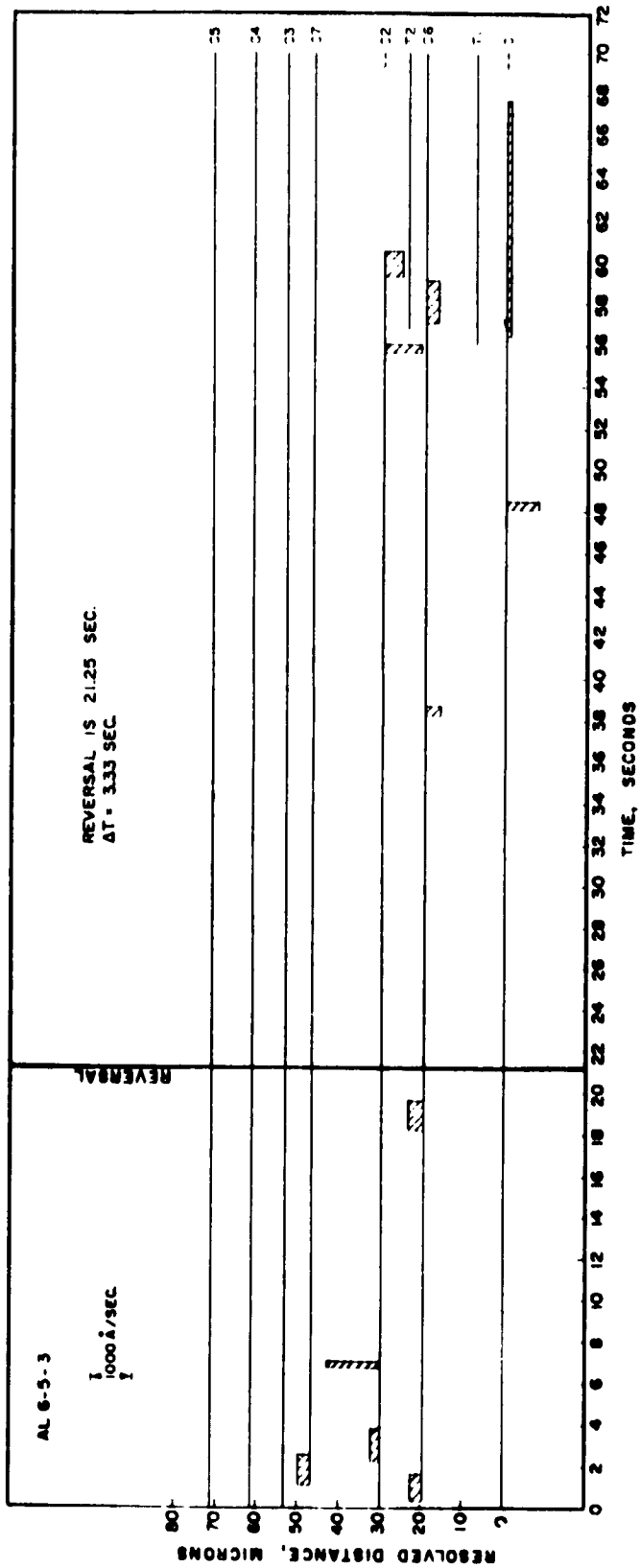
AL 6-5-3
1000 Å/SEC
REVERSAL
REVERSAL IS 21.25 SEC.
ΔT = 3.33 SEC.
RESOLVED DISTANCE, MICRONS
TIME, SECONDS

FIG. 9

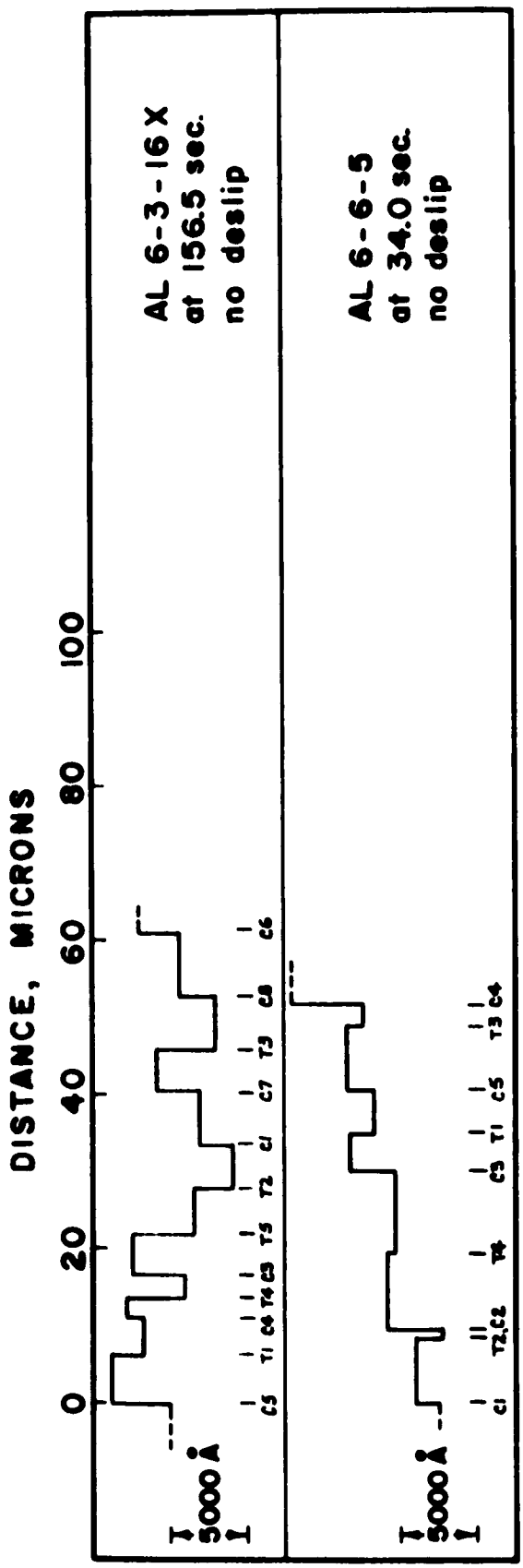
AL 6-3-16 X
at 156.5 sec.
no deslip
AL 6-6-5
at 34.0 sec.
no deslip
DISTANCE, MICRONS
0
20
40
60
80
100
5000 Å
5000 Å

FIG. 10

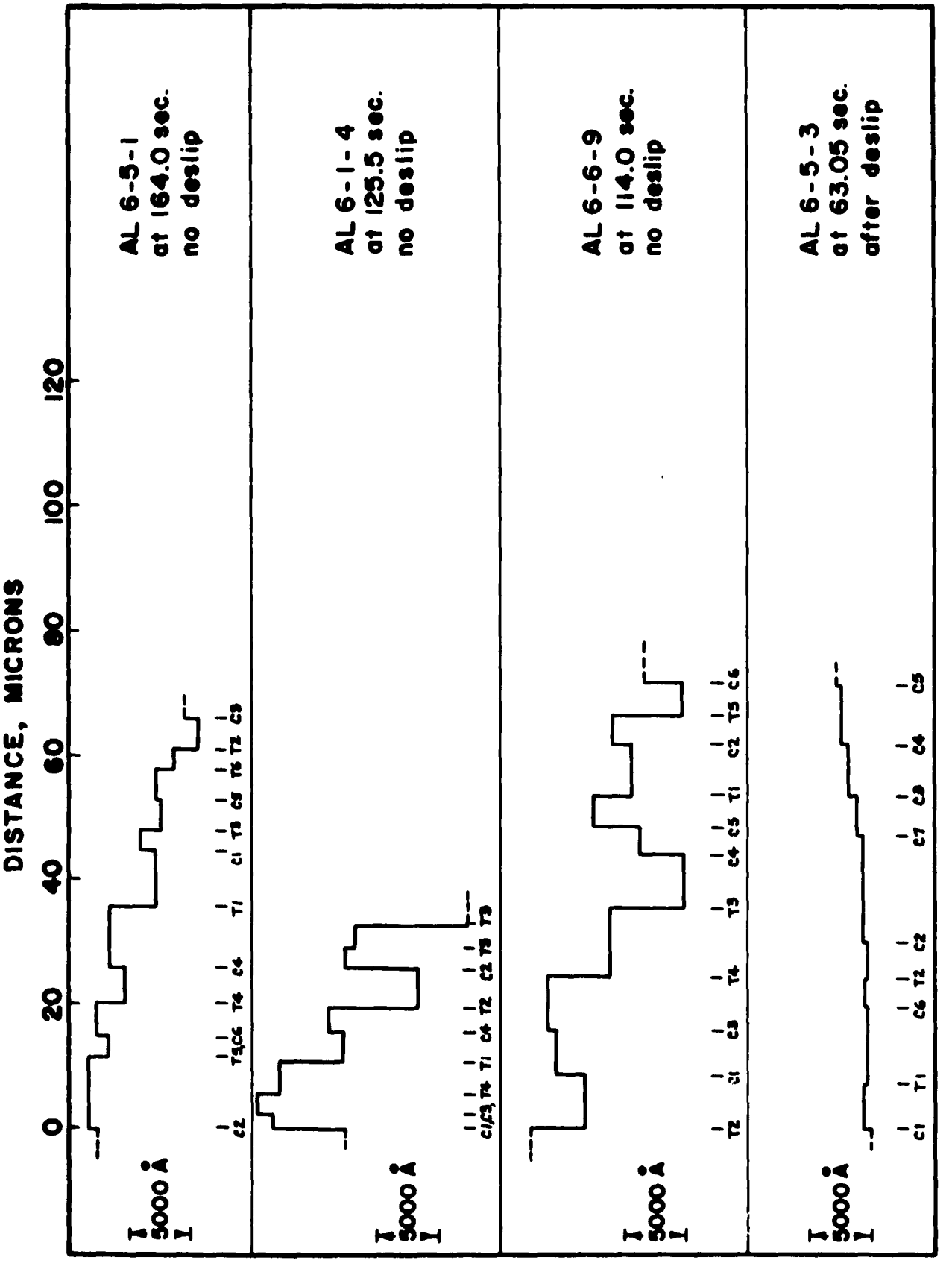
DISTANCE, MICRONS
0
20
40
60
80
100
120
AL 6-5-1
at 164.0 sec.
no deslip
AL 6-1-4
at 125.5 sec.
no deslip
AL 6-6-9
at 114.0 sec.
no deslip
AL 6-5-3
at 63.05 sec.
after deslip
5000 Å

FIG. 11

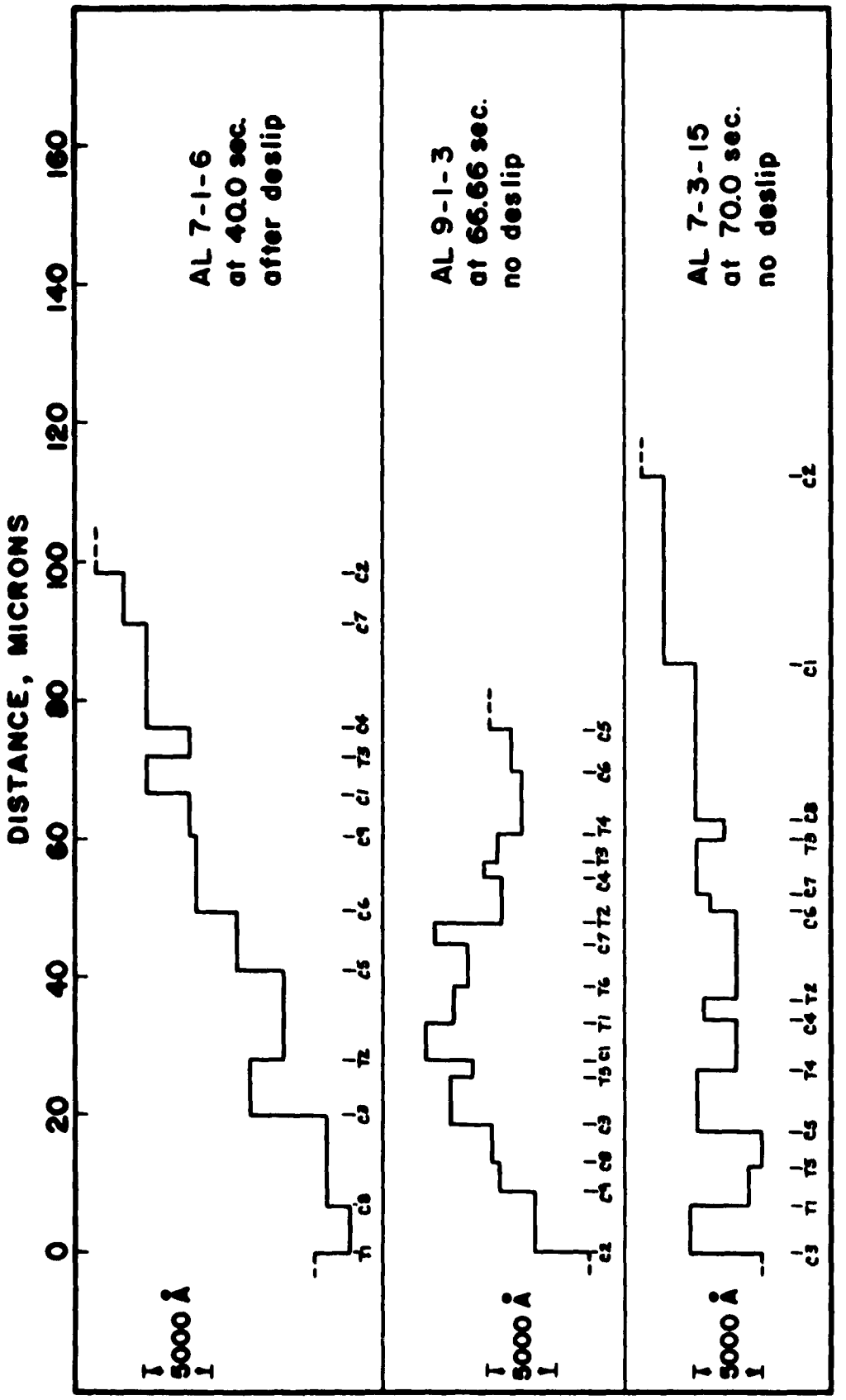
DISTANCE, MICRONS
0
20
40
60
80
100
120
140
160
AL 7-1-6
at 40.0 sec.
after deslip
AL 9-1-3
at 66.66 sec.
no deslip
AL 7-3-15
at 70.0 sec.
no deslip
5000 Å
5000 Å
5000 Å

FIG. 12

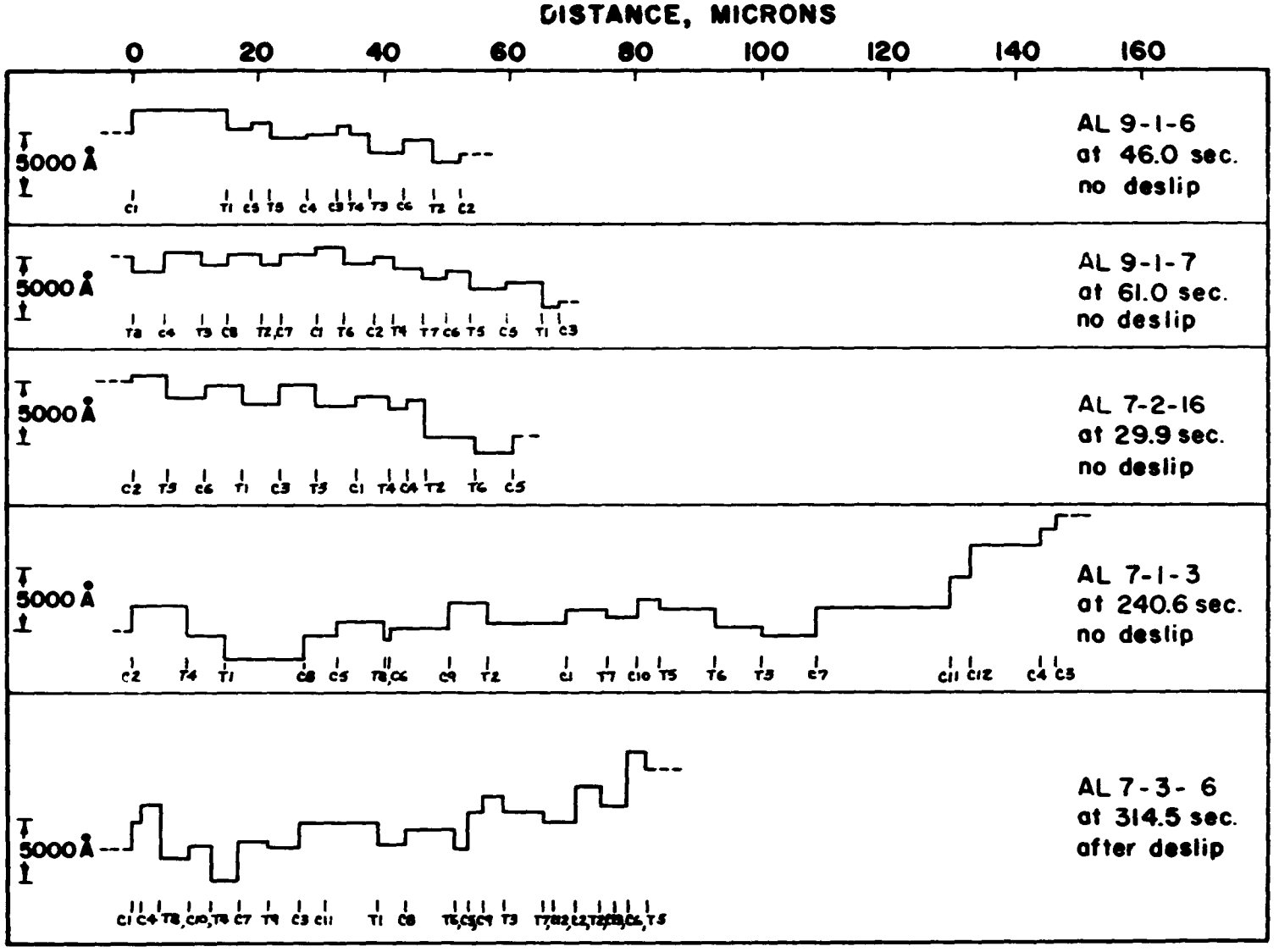
DISTANCE, MICRONS
0
20
40
60
80
100
120
140
160
5000 Å
AL 9-1-6
at 46.0 sec.
no deslip
5000 Å
AL 9-1-7
at 61.0 sec.
no deslip
5000 Å
AL 7-2-16
at 29.9 sec.
no deslip
5000 Å
AL 7-1-3
at 240.6 sec.
no deslip
5000 Å
AL 7-3-6
at 314.5 sec.
after deslip

FIG. 13

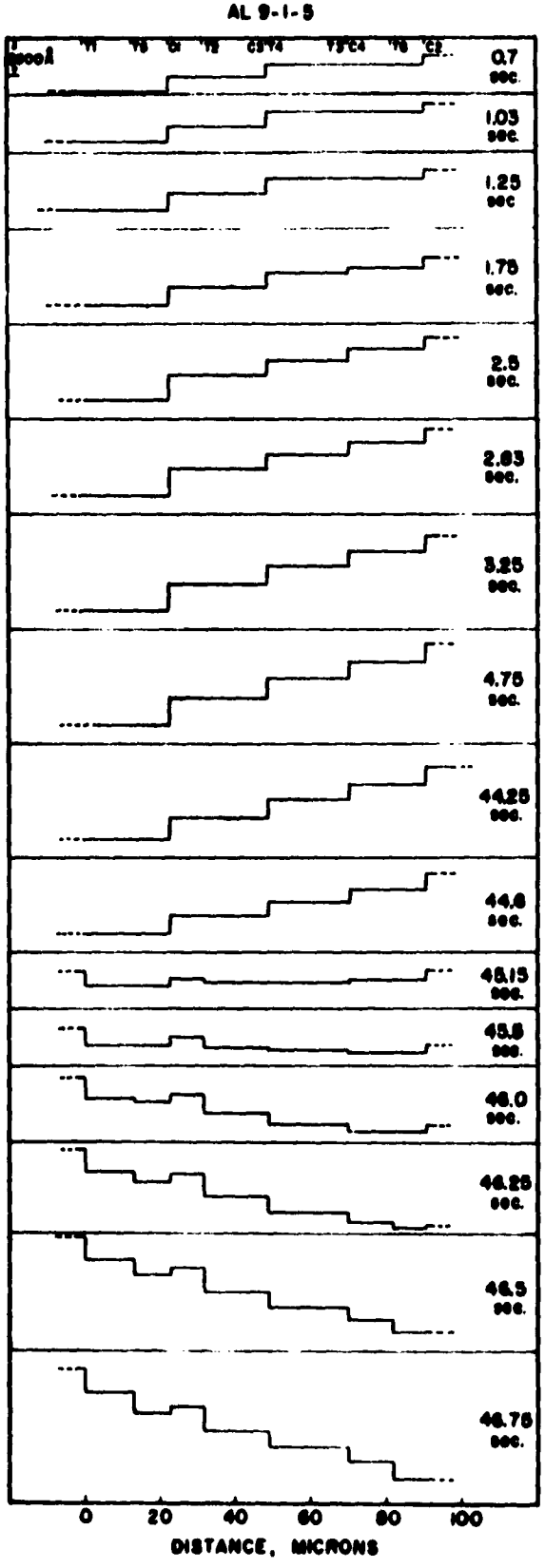
AL 9-1-5
0.7 sec.
1.03 sec.
1.25 sec
1.75 sec.
2.5 sec.
2.83 sec.
3.25 sec.
4.75 sec.
44.25 sec.
44.6 sec.
45.13 sec.
45.5 sec.
46.0 sec.
46.25 sec.
46.5 sec.
46.75 sec.
0
20
40
60
80
100
DISTANCE, MICRONS

FIG. 14

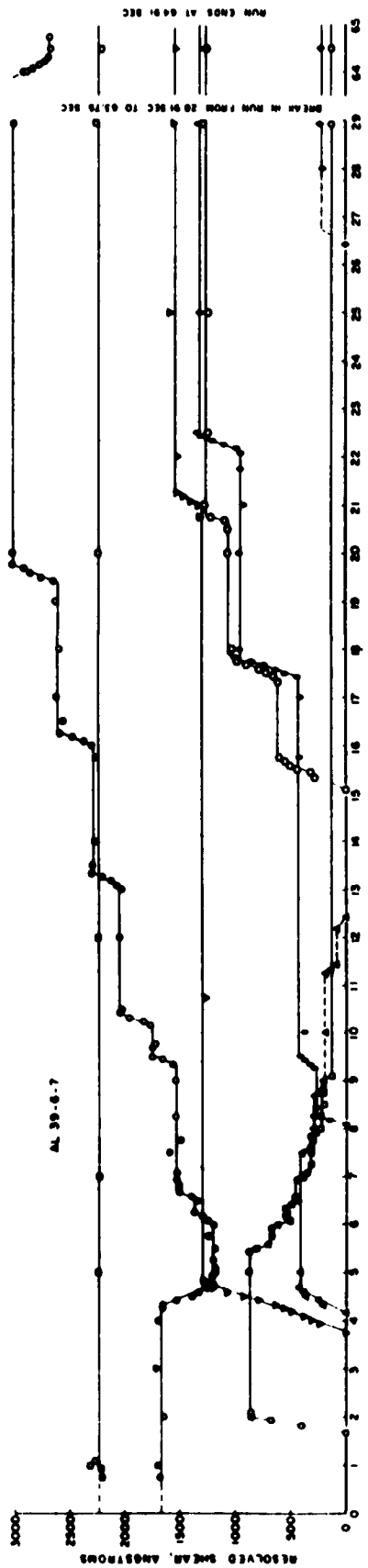
RUN ENDS AT 64.91 SEC
MEAN OF RUN FROM 20.91 SEC TO 63.78 SEC
AL 39-6-7
RESOLVED SHEAR, ANGSTROMS
TIME, SECONDS

FIG. 15

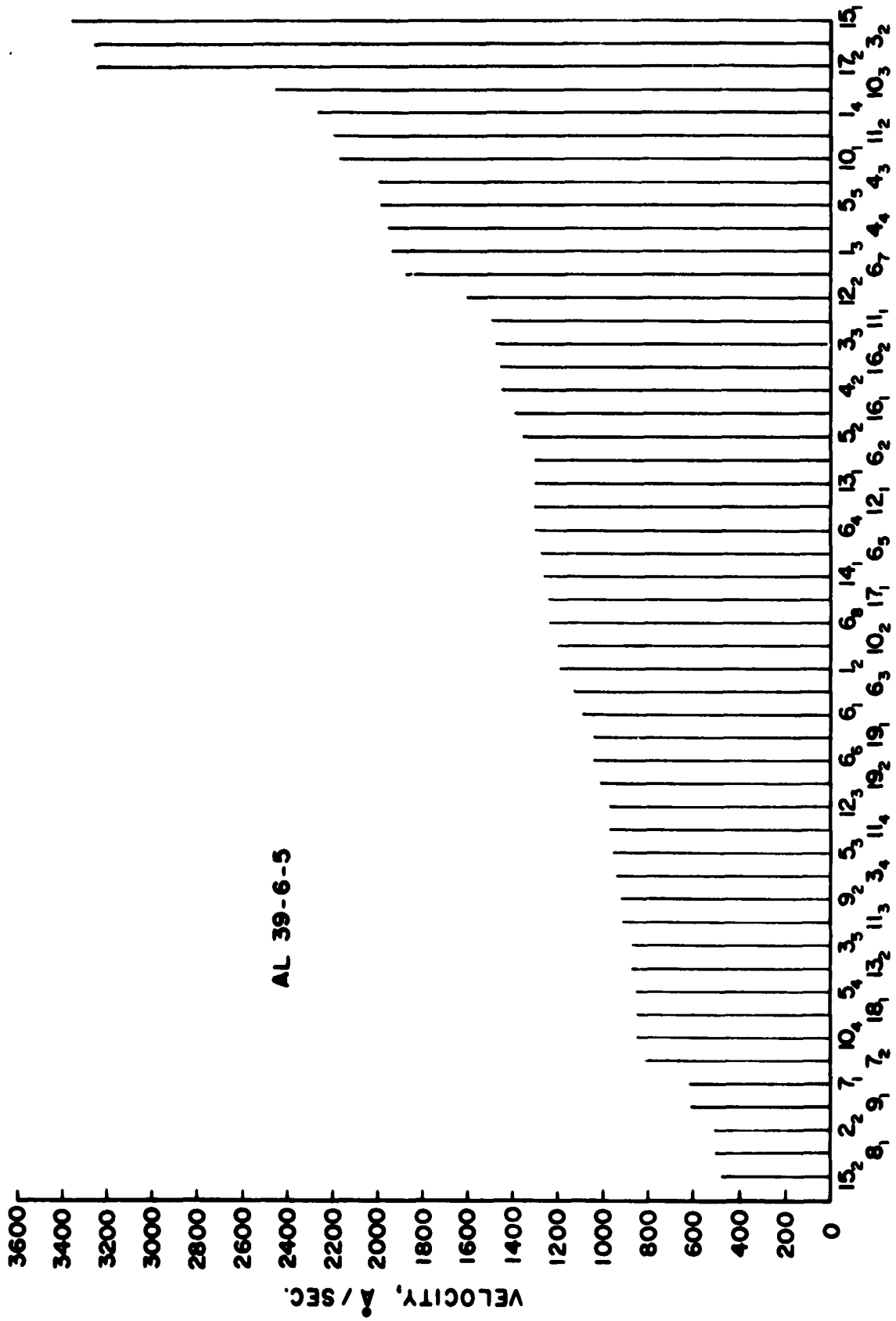
AL 39-6-5
VELOCITY, Å / SEC.
0
200
400
600
800
1000
1200
1400
1600
1800
2000
2200
2400
2600
2800
3000
3200
3400
3600
LINE NUMBER

FIGURE 16

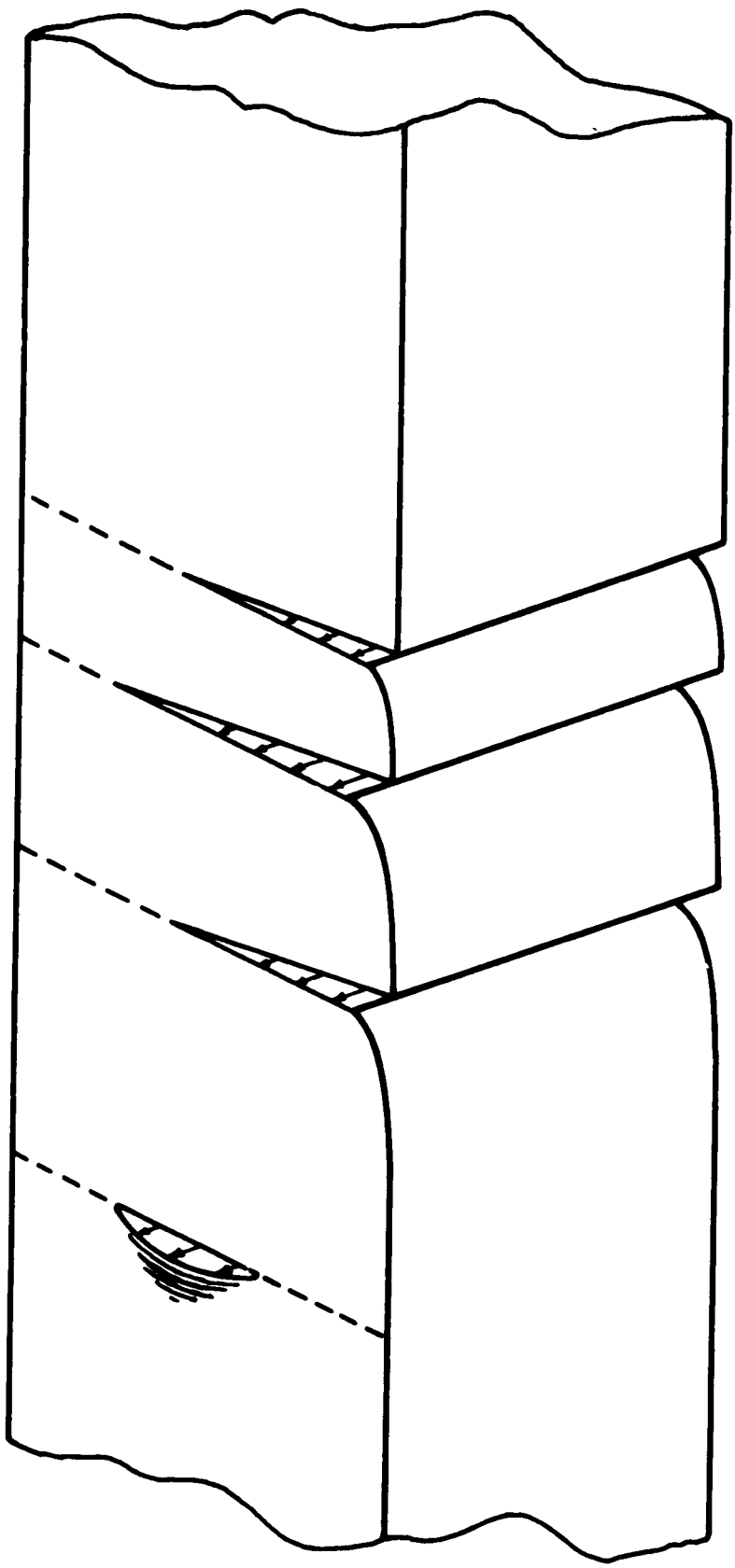

FIGURE 17

BIBLIOGRAPHY

1. N. K. Chen, R. B. Pond: "Dynamic Formation of Slip Bands in Aluminum," Trans. AIME Oct. 1952 p. 1085-1092.

2. R. Becker, P. Haasen: "Kinematographie Von Gleitlinien Auf Al.-Einkristallen" Acta Met 1 (1953) 325.

3. P. Haasen, R. Siems: "Wachstum Von Gleitlinien Auf Einkristallen Aus Aluminum Und Zink" Z Metallkunde, Vol. 48 (1957), p. 315-326.

4. R. B. Pond, E. Harrison: "Slip Velocities in Several Metals as Measured by Interferometric Cinemicrography" ASTIA Document No. AD 162 153, August 1958.

5. R. B. Pond, E. Harrison: "Cinemicrographic Recording of Multiple [illegible]m Interferometric Fringes during Plastic Deformation of Single Crystals," Review of Scientific Instruments, Vol. 28 (1957), p. 574.

DISTRIBUTION LIST FOR TECHNICAL NOTES AND TECHNICAL REPORTS

SOLID STATE SCIENCES DIVISION — 1 March 1961

AGENCY	NUMBER OF COPIES
Air Force Office of Scientific Research ATTN: Solid State Sciences Division Wash. 25, DC	3
Air Force Office of Scientific Research ATTN: Technical Library (SRGL) Wash. 25, DC	2
ASTIA (TIPCR) Arlington Hall Station Arlington 12, Va.	10
ARDC(RDRS) Andrews AFB Wash. 25, DC	1
EOAFRD ARDC 47 Cantersteen Brussels, Belgium	1
HQ USAF(AFDRT) Wash. 25, DC	1
ARL (Technical Library) Bldg. 450 Wright-Patterson AFB, Ohio	1
WADD(WWAD) Wright-Patterson AFB, Ohio	1
WADD (Metals & Ceramics Lab) Materials Central Wright-Patterson AFB, Ohio	
WADD (Physics Lab) Materials Central Wright-Patterson AFB, Ohio	1
WADD (Materials Information Branch) Materials Central Wright-Patterson AFB, Ohio	1
Institute of Technology (AU) Library MCLI-LIB, Bldg. 125, Area B Wright-Patterson AFB, Ohio	1

ARL (Metallurgy) 1
AFRD
Wright-Patterson AFB, Ohio

ARL (Physics, Solid State) 1
AFRD
Wright-Patterson AFB, Ohio

AFOSR (SRLTL) 1
Holloman AFB, New Mexico

AFCRL (CRRELA) 1
Laurence G. Hanscom Field, Bedford, Mass.

AFFTC (FTCTL) 1
Edwards AFB, California

AEDC (AEOIM) 1
Arnold Air Force Station, Tennessee

AFSWC (SWOI) 1
Kirtland AFB, New Mexico

Commander 2
Army Rocket & Guided Missile Agency
ATTN: ORDXR-OTL
Redstone Arsenal, Alabama

Office of the Chief of Research and Development 1
Department of the Army
ATTN: Scientific Information
Washington 25, D. C.

Army Research Office (Durham) 1
ATTN: CRD-AA-IP
Box CM, Duke Station
Durham, North Carolina

Commanding Officer 1
Ordnance Materials Research Office (ATTN: PS&C Div.)
Watertown Arsenal
Watertown 72, Massachusetts

Commanding Officer 1
Watertown Arsenal
ATTN: Watertown Arsenal Labs, Tech Reports Section
Watertown 72, Massachusetts

Commander 1
Signal Corps Engineering Laboratory
ATTN: SIGFM/EL-ROP
Fort Monmouth, New Jersey

Director 1
US Naval Research Laboratory
ATTN: Library
Wash. 25, DC

Department of the Navy 2
Office of Naval Research
ATTN: Code 423
ATTN: Code 421
Wash. 25, DC

Officer in Charge 1
Office of Naval Research
Navy No. 100
Fleet Post Office
New York, New York

Commanding Officer 1
Naval Radiological Defense Laboratory
San Francisco Naval Shipyard
San Francisco 24, California

Dr. D. F. Bleil 1
Associate Technical Director for Research
US Naval Ordnance Lab
White Oak, Silver Spring, Maryland

National Aeronautics & Space Agency 1
ATTN: Library
1520 H St., N. W.
Wash. 25, DC

Ames Research Center (NASA) 1
ATTN: Tech Library
Moffett Field, California

High Speed Flight Station (NASA) 1
ATTN: Tech Library
Edwards AFB, California

Langley Research Center (NASA) 1
ATTN: Tech. Library
Langley AFB, Virginia

Lewis Research Center (NASA) 1
ATTN: Tech Library
21000 Brookpark Road
Cleveland 35, Ohio

Wallops Station (NASA) 1
ATTN: Tech Library
Wallops Island, Virginia

Division of Research
US Atomic Energy Commission
Division Office
Washington 25, D. C. — 1

US Atomic Energy Commission
Library Branch
Tech Information Div., ORE
P.O. Box #E
Oak Ridge, Tennessee — 1

Major John Radcliffe
ANP Office
US Atomic Energy Commission
Washington 25, D. C. — 1

Oak Ridge National Laboratory
ATTN: Central Files
Post Office Box P
Oak Ridge, Tennessee — 1

Brookhaven National Laboratory
ATTN: Research Laboratory
Upton, Long Island, New York — 1

Argonne National Laboratory
ATTN: Librarian
9700 South Cass Avenue
Argonne, Illinois — 1

Document Custodian
Los Alamos Scientific Laboratory
P. O. Box 1663
Los Alamos, New Mexico — 1

Ames Laboratory
Iowa State College
P. O. Box 14A, Station A
Ames, Iowa — 1

Knolls Atomic Power Laboratory
ATTN: Document Librarian
P.O. Box 1072
Schenectady, New York — 1

National Science Foundation
1901 Constitution Avenue., N. W.
Washington 25, D. C. — 1

National Bureau of Standards Library
Room 203, Northwest Building
Washington 25, D. C. — 1

Director 1
Office of Technical Services
Department of Commerce
Technical Reports Branch
Washington 25, DC

Chairman 1
Canadian Joint Staff (DRB/DSIS)
2450 Massachusetts Avenue, N. W.
Washington, DC

Defense Research Member 1
Canadian Joint Staff
ATTN: Mr. H. C. Oatway
Director of Engineering Research
Defense Research Board
Ottawa, Canada

Institute of the Aeronautical Sciences 1
ATTN: Librarian
2 East 64th Street
New York 21, New York

RAND Corporation 2
1700 Main Street
Santa Monica, California